Available online at www.sciencedirect.com

ScienceDirect

Procedia Engineering 90 (2014) 631 – 636

Procedia Engineering

www.elsevier.com/locate/procedia

10th International Conference on Mechanical Engineering, ICME 2013

Neural network modeling and analysis for surface characteristics in electrical discharge machining

Md. Ashikur Rahman Khan[a,*], M. M. Rahman[b], K. Kadirgama[b]

[a]*Department of Information and Communication Technology, Noakhali Science and Technology University, Noakhali-3814, Bangladesh*
[b]*Faculty of Mechanical Engineering, Universiti Malaysia Pahang, 26600 Pekan, Pahang, Malaysia*

AbstractThe problem appeared owing to selection of parameters increases the deficiency of electrical discharge machining (EDM) process. Modelling can facilitate the acquisition of a better understanding of such complex process, save the machining time and make the process economic. Thus, the present work emphasizes the development of an artificial neural network (ANN) model for predicting the surface roughness (R_a). Trainingandtestingaredonewithdatathatarefoundsucceedingtheexperimentasdesignofexperiments. The surface topography of the machined part was analysed by scanning electronic microscopy. The result shows thatthe ANN model can predict the surface roughness effectively. Low discharge energy level results in smaller craters and micro-cracks producing a suitable structure of the surface. This approach helps in economic EDM machining.

Selection and peer-review under responsibility of the Department of Mechanical Engineering, Bangladesh University of Engineering and Technology (BUET)

Keywords: Graphite; modelling; neural network; surface roughness; Ti-5-2.5.

1. Introduction

Titanium is used in many industries and commercial applications;however, titanium is a difficult-to-cut material for conventional machining process[1, 2]. A non-conventional technique, EDM can machine this hard material effectively [3].Electrical discharge machining process is highly complex and stochastic. The complicated mechanisms to the process result a lag of established formula correlating the input and output parameters. Modelling can solve the problem araised as of

Nomenclature

b	bias
h_j	value of the output for hidden nodes
I_p	peak current
R_a	surface roughness
S_v	servo-voltage
T_{on}	pulse-on time
T_{off}	pulse-off time
w_i	synaptic weight
x_i	input value

*Corresponding author.E-mail address: ashik.nstu@yahoo.com

Selection and peer-review under responsibility of the Department of Mechanical Engineering, Bangladesh University of Engineering and Technology (BUET)
doi:10.1016/j.proeng.2014.11.783

y_o	output for output nodes

parameter selection and make the process economic [4]. In recent years, the artificial neural network has been transformed into a very useful tool for modelling complex systems [5]. The first research to distinguish the EDM pulse type using artificialintelligence was carried out byKao and Tarng[6]. A feed-forward neural network (NN) was adopted to associate the relationships between tool-workpiece gap signals and various pulse types. Based on this model, EDM pulses under varying machining conditions could be classified quickly and accurately by measuring the voltage and current across the gap between the tool and the workpiece and feeding these data into the developed network. Mahdavinejad showed that there are four completely distinct pulses in EDM, and this system becomes unstable when the number of non-successive pulses, such as arcing, short circuit, and open circuit, is increased against normal discharges during the machining process [7]. Thus, the method of model predictive control based on ANN with output parameters of the system was used to minimize the number of non-successive pulses. Twodifferentartificialneuralnetworkmodels:backpropagationneuralnetwork(BPN)andradialbasisfunctionNNwerepresentedfor thepredictionofsurfaceroughness[8]. An investigation was carried out to study the effect of current and tool dimension on surface roughness for EDM machining [9]. The response variables were predicted using ANN techniques. Influences of EDM parameters on surface quality were analysed conducting the machining on cemented carbide[10].

It is seen that several studies have been conducted by using ANN for distinct materials such as SKD11 workpiece, 94WC–6Co, mild steel (St 37), alloyed steels (C 45 and 100Cr6), high strength low alloyed (HSLA) steels; mild steel, WC-Co, HE15, 15CDV6, and M250, AISID2steel [6,10, 11, 9, 7, 5, 12, 13, 8]. However, the development of the model for predicting surface roughness of Ti-5-2.5 work material in EDM process is still lagging. In this perspective, it is aimed to develop an ANN model that accurately correlates the EDM process variables as peak current, pulse-on time, pulse-off time, servo-voltage and performance, namely surface roughness (R_a) of Ti-5-2.5. The experimental work is carried out by using a numerically controlleddie-sinking EDM. The effect of the process parameters on R_a is studied as well. The surface topography of the machined surface has been analysed through scanning electronic microscope.

2. Research Methodology

2.1. Experimental procedure

In this research, the surface roughness (R_a) is considered as response parameter, and parameters such as peak current(I_p), pulse-on time(T_{on}), pulse-off time (T_{off}) and servo-voltage (S_v) are selected as EDM variables. The ranges of the process parameters were fixed carrying out the preliminary experiment. The cylindrical graphite electrodes with positive polarity were chosen as tool material. The process parameter ranges and machining condition for SEM viewing are presented in Table 1.The experimental work was conducted based on axial point central composite design (CCD) of response surface methodology. Machining was performed, varying I_p, T_{on}, T_{off}, and$S_v$according to the design matrix obtained through CCD. The value of surface roughness was assessed using the Perthometer. Five observations were carried out on different positions of the machined surface for each sample, and the average of these five was taken as the value of R_a. Surface texture analysis was carried out by scanning electronic microscopy (SEM) to observe the surface topography of selected specimens. The specimens were machined in EDM as per settings shown in Table 1(b), and were prepared for SEM viewing following EDM.

Table 1. (a) The process parameters and their ranges.

Process parameters	Range
Peak current (I_p)	1–29 A
Pulse-on time (T_{on})	10–350 µs
Pulse-off time (T_{off})	60–300 µs
Servo-voltage (S_v)	75–115 V

(b) Machining setting for SEM viewing.

Parameters	Setting-1	Setting-2	Setting-3
Peak current (I_p)	2	15	29
Pulse-on time (T_{on})	95	180	320
Pulse-off time (T_{off})	120	120	120
Servo-voltage (S_v)	85	85	85

2.2.Modelling

In the present work, feed forwardmultilayer perceptron neural network is applied and developed for predicting the surface roughness. A multiple input neuron model which consists of a single neuron with x_i inputs. In this case, the net input to the transfer function (f) and the output for the neuron can be is defined as follow

$$net\_input = \sum_{i=1}^{n} w_i x_i + b\,; \qquad output = f(\text{net\_input}) \tag{1}$$

Here, w_i is the synaptic weight, and b is the bias. The MLP neural network is formed from numerous neurons with parallel connections, which are joined in several layers [5]. In this research effort a number of networks are constructed, altering numbers of hidden layers, the number of hidden neurons, maximum epochs, training repetition, and momentum factor, and

each of them is trained separately.A model with one hidden layer was found more satisfactory. Accordingly, MLP feed-forward neural network models with one hidden layers were developed. The network structure can be defined as 4-*j*-1. The four nodes for the input layer (I_p, T_{on}, T_{off}, and S_v),and one nodefor the output layer transmitsR_a. According to Eq. (1), the net input to unit *j* in the hidden layer,and the net input to unit *o* in the output layer can be expressed in Eq. (2),

$$(net\_input)_{hidden}=\sum_{i=1}^{I} w_{i,j}x_i + b_j \; ; \qquad (net\_input)_{output}=\sum_{j=1}^{J} w_{j,o}h_j + b_o \tag{2}$$

where $w_{i,j}$ is the weight between the input neurons and hidden neurons; x_i is the value of the input as $x_1=I_p$, $x_2=T_{on}$, $x_3=T_{off}$, and $x_4=S_v$; b_j is the bias on the hidden nodes; $w_{j,o}$ is the weight between the hidden and output neurons, h_j is the value of the output for hidden nodes, and b_o is the bias on the output nodes. As Eq. (2), the output for hidden nodes, and the output for output nodes (y_o) can be given as Eq. (3),

$$h_j=f((net\_input)_{hidden}) \; ; \qquad y_o=f((net\_input)_{output}) \tag{3}$$

Where f is the transfer function and y_o is the ANN predicted output, namely, R_a. According to the sigmoid function, the transfer function can be written as $f(\text{net})=1/(1+e^{-\text{net}})$. Therefore, the output for hidden nodeswith the sigmoid function, and the output for output nodes with the sigmoid function can be written as Eq. (4) combining Eq. (2) and Eq. (3).

$$h_j = f((net\_input)_{hidden})=\frac{1}{1+ e^{-\sum_{i=1}^{I} w_{i,j}x_i + b_j}} \; ; \qquad y_o = f((net\_input)_{output})=\frac{1}{1+ e^{-\sum_{j=1}^{J} w_{j,o}h_j + b_o}} \tag{4}$$

Eq. (4) can be expressed for the ANN predicted R_a as Eq. (5).

$$R_a=\frac{1}{1+ e^{-\sum_{j=1}^{J} w_{j,o}h_j + b_o}} \tag{5}$$

A trial-and-error approach was used to ascertain the optimal structure. The selected best neural network model is trained (three times), substituting the set of the training data acquired from the experimental results. Testing was performed using experimental data that were not used for training purposes.The validation of the ANN model was performed using production data that comprises input data only. The impact of the process parameters on surface roughness was investigated. For this analysis, in each stage only one input parameter randomly changes between its minimum and maximum duration, while the others are fixed in their reference condition [14].

3. Results and Discussion

3.1.Modelling

Table 2. Performance of neural network with different architectures.

Observation no.	No. of hidden layer	Network structure	Momentum factor	No. of training repetitions	Max no. of epochs	MSE	r-value
1	2	4-8-5-1	0.4	3	50000	3.39×10^{-5}	0.8789
2	2	4-7-6-1	0.5	2	40000	4.51×10^{-4}	0.8831
3	1	4-10-1	0.4	3	60000	1.67×10^{-5}	0.9427
4	3	4-7-5-4-1	0.4	3	60000	9.34×10^{-4}	0.8049
5	2	4-6-9-1	0.6	2	30000	6.13×10^{-4}	0.9021
6	2	4-10-5-1	0.5	3	50000	2.22×10^{-5}	0.8942
7	3	4-8-10-4-1	0.7	2	40000	3.91×10^{-4}	0.7084
8	2	4-8-4-1	0.4	3	60000	5.64×10^{-5}	0.7559
9	2	4-8-4-1	0.5	2	50000	4.24×10^{-4}	0.8591
10	1	4-12-1	0.5	3	30000	6.17×10^{-5}	0.7947
11	2	4-6-9-1	0.6	1	30000	8.13×10^{-5}	0.8302
12	1	4-12-1	0.5	3	60000	8.24×10^{-5}	0.6903
13	3	4-9-6-4-1	0.5	2	50000	1.50×10^{-4}	0.8561
14	2	4-6-4-1	0.5	3	50000	1.62×10^{-4}	0.6940
15	2	4-6-4-1	0.5	1	60000	8.31×10^{-5}	0.7938
16	3	4-7-5-4-1	0.5	3	30000	1.48×10^{-3}	0.8357
17	2	4-9-6-1	0.5	3	50000	1.92×10^{-5}	0.9534
18	1	4-12-1	0.5	3	50000	9.02×10^{-6}	0.8007
19	1	4-9-1	0.5	2	40000	8.21×10^{-5}	0.8807
20	3	4-9-6-4-1	0.5	3	60000	1.50×10^{-3}	0.8613

The prediction capability of different architecture is shown in Table 2. It is noticed that the observation 18 yields the

lowest value of MSE as 9.02×10^{-6} but its linear correlation coefficients (r-value) is lower (0.8007). On the other hand, observations 3 and 17 offer suitable value of MSE (1.67×10^{-5} and 1.92×10^{-5}) and r-value (0.9427 and 0.9534). It is noticed that the r-value of observation 3 and 17 is almost similar however; the observation 3 yields lower value of MSE. Accordingly, the neural network architecture for observation number 3, which is 4-10-1 (one hidden layer with 10 neurons), is chosen as the best network in predicting R_a. Henceforth,the training is stopped and the weight values of the NNare stored.

In testing of the NN model, the performance measures such as mean square error as well as the linear correlation coefficient of the model are found as 0.0439 and 0.9727, respectively. Thus, it is apparent that the linear correlation coefficient obtained (0.9727) is satisfactory. It is also observed that the MSE (0.0439) obtained are within the acceptable range. To investigate the line pattern of the data between the target values and ANN outputs (from training and testing) two lines are generated on the same graph as shown in Fig.1. It is found that the predicted and experimental values are very close to each other and the patterns of the two lines are identical except for a few data points. Thus, there is good agreement between the experimental values and neural network outputs.The regression analysis between the network response and the corresponding experimental value are presented in Fig. 2. Approximately all the points on the plot come close to forming a straight line, which signifies that the data are normal. According to this figure the value of R^2 (0.9371) is over 90%, which indicates a very good correlation between the ANN model predicted value and the experimental value. Therefore, the developed neural network model is adequate to illustrate the pattern of surface roughness in EDM process.

The results for confirmation tests (Table 3) indicates that the error between the observed value and the ANN output is in the range of 1.77—2.95% with an average errors of 1.92%. Thus, it is obvious that the error is within the agreeable limit and the accuracy of the developed model representing R_a is satisfactory.

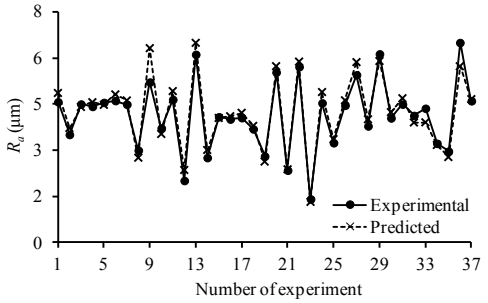

Fig. 1. Comparison between ANN predicted and experimental values.

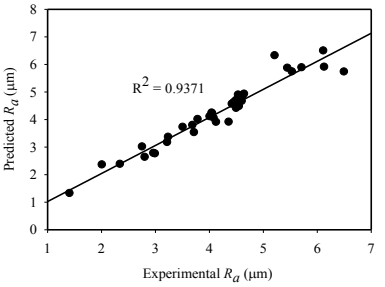

Fig. 2.Predicted versus experimental surface roughness.

Table 3: Error analysis for the ANN model of surface roughness.

Electrode	Polarity	Experimental R_a (μm)	ANN PredictedR_a (μm)	Error (%)	Average error
Graphite	Positive	6.3396	6.4516	1.77	
		5.1220	5.0680	1.05	1.92
		2.4047	2.3337	2.95	

3.2.Impact of process parameters

The impact of the I_p on the R_a is shown in Fig. 3. It is apparent from Fig. 3(a) that the $R_a$increases graduallyupto15 Aandbeyondthisrange,adisparatecharacteristicofR_a isappearedwiththeincreaseofI_p. The increase of $I_p$increases the discharge energy, which promotes melting and vaporization of the workpiece material and generates larger and deeper craters, thus producing a higher R_a. The crater size increases with an increase of current, and ultimately the surface finish becomes rougher. The$R_a$alsodependsontoolwear,andthelowertoolcauseslowerR_a. In EDM, carbon cracked from kerosene deposits on the electrode surface and forms a protective layer during machining. A black carbon layer is observed on the surface of the flat portion caused by the growth of attached carbon from cracked kerosene dielectric carbon oil [15]. This carbon layer protects the surface of the electrode from spark erosion. The increase of peak current tends to increase the carbon layer which tends to decrease the tool wear. Thus,thehighpeakcurrent(>23A) causes a decreasing trend of the R_a.

It is seen that initially the R_a increases until a specific (peak) value and then retain constant when the T_{on} increases, as shown in Fig. 3(b). As the T_{on} increases the discharge energy increases. The high discharge energy creates more craters enhancing material erosion. Therefore, the R_a increases as the T_{on} increases. However, the too long T_{on}causes arcing and reduces the material erosion. The energy density within the discharge spot is reduced on account of the expansion of discharge column at a longer T_{on}. As a result, small craters are produced at too long T_{on}. Thus, the decreasing tendency is apparent to too long T_{on}(about 280–350 μs).

As can be seen from the Fig. 3(c) the diverse impact of the pulse-off time on surface roughness characteristics is apparent in this study. An increasing of T_{off} initially increases R_a, and thereafter reduces R_a. When the T_{off} is short, there is not enough

time to clear the disintegrated particles from the gap between the electrode and the workpiece. If the T_{off} is short, an unstable spark discharge can be easily induced because of insufficient insulation recovery. Therefore, the short T_{off} results higher R_a, and R_a decreases with the increase of T_{off}. The pulse-off time must be sufficiently long to acquire a uniform erosion of material from the surface of the workpiece and stable machining process; otherwise, a non-uniform erosion of the workpiece surface will occur. Thus, disparate effects of pulse-off time on surface finish have been observed.

It is apparent from Fig. 3(d) that as the S_v increases the R_a decrease. At high servo-voltage, the electrode is no longer able to advance towards the workpiece, resulting in a decrease in discharge. Besides, high servo-voltage allows lower time for the cutting operation. Thus, an increase in S_v reduces the material erosion resulting in small size of craters. Therefore, the R_a decreases with an increase of S_v, and a higher value of servo-voltage presents a more even surface on the workpiece.

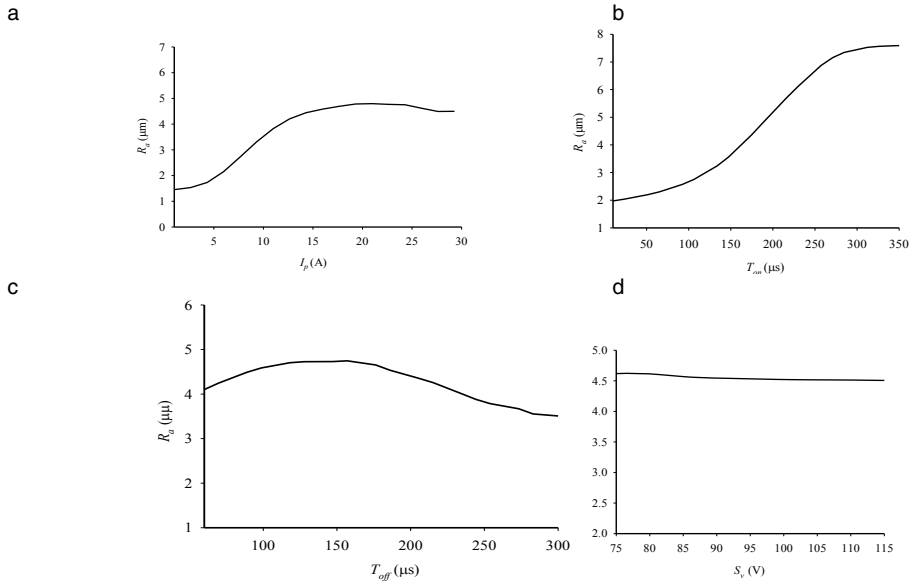

Fig. 3. (a) Effect of I_p on R_a; (b) effect of T_{on} on R_a; (c) effect of T_{off} on R_a; (d) effect of S_v on R_a.

4.Surface topography

The surface topography of a number of samples (table 2) is investigated using scanning electronic microscopy of the machined surface. The surface topography of the machined surface generated during EDM with positive graphite electrode is illustrated in Fig. 4 for distinct discharge energy. These figures exhibit globules, craters, cracks, and small debris on the machined surface.The spark occurring through the high-temperature plasma melts and vaporizes a small area of the workpiece surface, and ultimately craters are formed. The crater size depends on the peak current as well as the discharge energy. Small craters are produced at low peak current. Low peak current and high frequency correspond to low material erosion, which results in smaller craters. Scanning electronic micrographs reveals the presence of cracks resulting from solidification and/or rapid cooling of the recast layer. Many surface imperfections in the recast layer produced by the EDM process initiate cracking. At the end of discharge, the surface layer is rapidly cooled by the dielectric fluid and develops a residual tensile stress. Cracks are formed when the residual tensile stress in the surface exceeds the ultimate tensile strength of the material. The cracks are not readily formed within a thin recast layer because it is able to dissipate heat rapidly. Therefore, lower discharge energy produces micro-cracks. At the end of pulse-on time, a small amount of molten material is not expelled, although most of the melted and vaporized material is flushed away by the dielectric. The unexpelled melted material resolidifies after rapid cooling by the dielectric fluid and forms globules of debris.

According to the SEM images in Fig. 4, the size of the craters increase as the discharge energy level increases. It is revealed that the number of globules decreases as the energy level increases.In addition, the degree of cracks increases as the discharge energy increases. The large discharge energy causes violent sparks and impulsive force, which strike the surface. Therefore, the rate of melting and vaporization is increased, resulting in greater material removal. This produces larger and deeper craters on the machined surface of workpiece. The long T_{on} is responsible for larger craters however; strong I_p causes deep craters during high energy level. Therefore, high discharge energy produces deeper and wider craters, resulting in a rougher surface. The two factors that lead to a greater degree of crack formation are recast layer thickness and induced stress. The thickness of the recast layer increases with discharge energy. The increase in T_{on} increases the white layer thickness and residual stress. A larger amount of heat energy penetrates into the interior of the workpiece at long T_{on}. The temperature of the workpiece surface reaches the melting point readily. The molten material resolidifies following rapid cooling by the

dielectric fluid and produces a thick recast layer. Thus, the high energy level produces a greater degree of cracks. The high discharge energy produces an inhibitor carbon layer on the electrode surface. The amount of carbon accumulated on the electrode surface increases considerably according to the increase of T_{on}. This carbon layer diminishes the electrode wear. The high discharge energy causes a large impulsive force, which can remove more debris from the machining gap. Thus, the surface topography with high discharge energy reduces the amount of globules.

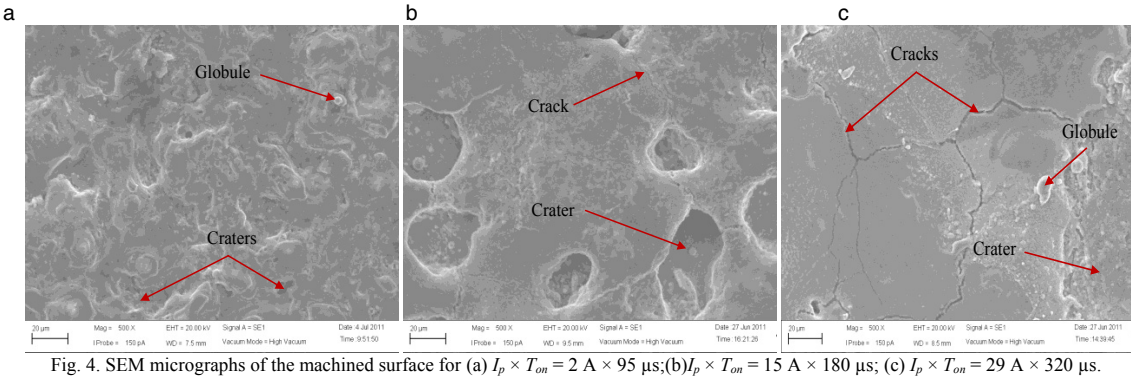

Fig. 4. SEM micrographs of the machined surface for (a) $I_p \times T_{on}$ = 2 A × 95 µs;(b)$I_p \times T_{on}$ = 15 A × 180 µs; (c) $I_p \times T_{on}$ = 29 A × 320 µs.

5. Conclusion

The important findings from the work carried out in this research are summarised in this section. The error is within the agreeable limit and the developed neural network model is adequate for prediction the surface roughness, R_a. As the I_p increases initially the surface roughness increases upto15 Aof $I_p$afterwards adisparatecharacteristicofR_a isappeared. A decreasing trend of the $R_a$is appeared at highI_p (>23A). It is found that the $R_a$increases with T_{on} however, the decreasing tendency is apparent to too long T_{on} (about 280–350 µs). The diverse impact of T_{off} on surface roughness (preliminary increasing and thereafter reducing tendency of R_a) characteristics is evident in this study. A higher value of $S_v$yields more even surface.Low peak current as well as low discharge energy level results in smaller craters and micro-cracks. On the other hand, high discharge energy produces higher degree of craters as well as greater degree of cracks, generating a rougher surface. The fine microstructure of the machined surface is gained with low discharge energy.

References

[1] M.A.R. Khan, M.M. Rahman, K. Kadirgama,Mathematical model and optimization of surface roughness during electrical discharge machining of Ti-5Al-2.5Sn with graphite electrode, Adv. Sci. Lett. 14 (2012) 879–884.
[2] M.A.R. Khan, M.M. Rahman, K. Kadirgama, R.A. Bakar, Artificial neural network model for material removal rate of Ti-15-3 in electrical discharge machining, Energy Edu. Sci. Tech. Part A: Energy Sci. Res. 29(2) (2012) 1025–1038.
[3] M.A.R. Khan, M.M. Rahman, K. Kadirgama, M.A. Maleque, R.A. Bakar, Artificial Intelligence Model to Predict Surface Roughness of Ti-15-3 Alloy in EDM Process,World Acad. Sci. Eng. Tech. 74 (2011) 121–125.
[4] R. Karthikeyan, P.R.L. Narayanan, R.S. Naagarazan, Mathematical modelling for electric discharge machining of aluminium–silicon carbide particulate composites, J. Mater. Process. Tech. 87 (1999) 59–63.
[5] R.A. Mahdavinejad, EDM process optimisation via predicting a controller model, Arch. Comput. Mater. Sci. Surface Eng. 1(3) (2009) 161–167.
[6] J.Y. Kao, Y.S. Tarng, A neutral-network approach for the on-line monitoring of the electrical discharge machining process. J. Mater. Process. Tech. 69 (1997) 112–119.
[7] R.A. Mahdavinejad, Optimisation of electro discharge machining parameters, J. Achievements Mater. Manuf. Eng. 27(2) (2008) 163–166.
[8] H.S. Nogay, T.C. Akinci, E. Guseinoviene, Determination of effect of slot form on slot leakage flux at rotating electrical machines by the method of artificial neural Networks,Energy Edu. Sci. Tech. Part A: Energy Sci. Res. 29 (2012) 451–462.
[9] H.K. Dave, K.P. Desai, H.K. Raval, Investigations on prediction of MRR and surface roughness on electro discharge machine using regression analysis and artificial neural network programming, Proceedings of the world congress on engineering and computer science, 2008.
[10] I. Puertas, C.J. Luis, L. Alvarez, Analysis of the influence of EDM parameters on surface quality, MRR and EW of WC–Co, J. Mater. Process. Tech. 153–154 (2004) 1026–1032.
[11] A.P. Markopoulos, D.E. Manolakos, N.M. Vaxevanidis, Artificial neural network models for the prediction of surface roughness in electrical discharge machining, J.Intell. Manuf. 19 (2008) 283–292.
[12] G.K.M. Rao, G.R. Janardhana, D.H. Rao, M.S. Rao, Development of hybrid model and optimization of metal removal rate in electric discharge machining using artificial neural networks and genetic algorithm, ARPN J. Eng. Appl. Sci. 3(1) (2008) 19–30.
[13] G.K.M. Rao, G. Rangajanardhaa, D.H. Rao, M.S. Rao, Development of hybrid model and optimization of surface roughness in electric discharge machining using artificial neural networks and genetic algorithm, J. Mater. Process. Tech. 209 (2009) 1512–1520.
[14] J. Ghaisari, H. Jannesari, M. Vatani, Artificial neural network predictors for mechanical properties of cold rolling products, Adv. Eng. Softw. 45 (2012) 91–99.
[15] N. Mohri, M. Suzuki, M. Furuya, N. Saito, Electrode wear process in electrical discharge machining, CIRP Annals - Manufacturing Technology. 44(1) (1995) 165–168.